



NAPROXEN: A CHALLENGING APPROACH FOR SOLIDLIPID NANOPARTICLES, DOSAGE FORM DESIGN, DEVELOPMENT AND EVALUATION OF BCS-II DRUGS

Adarsh Kumar Singh^{1*} and Prof. Dr. Pranav Kumar Upadhyay

¹Shri College of Pharmacy, Gaihat Ayer Varanasi.

Article Received on
12 June 2022,
Received on 02 July 2022,
Accepted on 23 July 2022
<http://www.journalwpr.com>

*Corresponding Author:
Adarsh Kumar Singh
Shri College of Pharmacy,
Gaihat Ayer Varanasi

ABSTRACT

Nanoparticle is the simplest form of structure with sizes in the nm range. In principle any collection of atoms bonded together with a structural radius of ≤ 100 nm can be considered a nanoparticle. In the present time nanoparticle are widely used in many dosage forms due to their good solubility, low size and better penetrability. Nanoparticle can be prepared by using the various methods such as Emulsion-Schwert Preparation Method, Double Emulsion and Emulsion Method, Salting out Method, Emulsion Diffusion Method, Solvent Displacement Precipitation method, Polymerization method and Coacervation or ionic gelation method. Applications of nanoparticle in micro wiring are cell specific, mineralization, vaccine delivery and gene delivery. Nanoparticles are used in the field of medicines also for the treatment of cancer or for the orthopaedic implants. Nanoparticles show high solubility and fast penetration that's why they are used in almost formulation now a day.

KEYWORDS: Gold Nanoparticle (AuNPs), Magnetic Resonance Imaging (MRI), Polyvinylpyrrolidone (PVP), Blood brain barrier (BBB)

INTRODUCTION

In today's drug development world, combinatorial chemistry, high-throughput screening, and genomics have provided a technologic platform that produces a large number of new chemical entities (NCE) with therapeutic potential each year. The pharmaceutical drug delivery market is also expected to grow from \$1048.1 billion in 2015 to \$1504.7 billion by 2020, with a compound annual growth rate of 7.5%. Despite a vast number of novel drug

molecules developed, only a few of them are successfully launched in the market (Poonia et al. 2016).²⁴ Because discovering and developing a drug is a time consuming and costly process with a recent estimation of about 13 years and US\$500 million, respectively. As well, the lack of efficacy (accounting for ~30% of failures), safety/toxicology and safety accounting for ~30%, low bioavailability and adverse pharmacokinetic profile (accounting for ~40%) were the prime reason for failure in the clinic. Hence, most drug candidate molecules are withdrawn before reaching clinical evaluation. Also, the newly discovered drugs from the discovery and development processes are not suitable for oral delivery (Lipinski et al. 2001).²⁵ Because the properties of new chemical entities shifted towards higher molecular weight and increasing lipophilicity. Consequently, the poor aqueous solubility of the lipophilic compounds has become an enduring problem in drug discovery as well as the early and late stage pharmaceutical development process. Also, it was reported that ~40% of currently marketed drugs and up to 70% of compounds currently under development had been suggested to be poorly water-soluble. As a result, an insufficient amount of drug reaches the systemic circulation followed by the site of action with a lack of pharmacological action and produce poor bioavailability (Poonia et al. 2016).²⁶

MATERIAL AND METHODS

Naproxen (M=230.2 g/mol) were purchased from Dharmic Pharma and Consultants, Mumbai, India. Naproxen were used without any further purification.

Drug	Naproxen
Structure:	
Orphan:	Approved, Investigational
Molecular Weight:	Average: 230.26
Chemical Formula:	C ₁₄ H ₁₆ O ₃
Pharmacology:	Naproxen is an established non-selective NSAID and is useful as an analgesic, anti-inflammatory and antipyretic.
Solubility:	It is lipid soluble, practically insoluble in water with a low pH (below pH 4), while freely soluble in water at 6 pH and above.
XLogP3:	3.3
Toxicity:	Although the over-the-counter (OTC) availability of naproxen provides convenience to patients, it also increases the

	likelihood of overdose. Thankfully, the extent of overdose is typically mild with adverse effects normally limited to drowsiness, lethargy, epigastric pain, nausea and vomiting.
	As with other non-selective NSAIDs, naproxen exerts its clinical effects by blocking COX-1 and COX-2 enzymes leading to decreased prostaglandin synthesis. Although both enzymes contribute to prostaglandin production, they have unique functional differences. The COX-1 enzyme is constitutively active and can be found in normal tissues such as the stomach lining, while the COX-2 enzyme is inducible and produces prostaglandins that mediate pain, fever and inflammation. The COX-2 enzyme mediates the desired antipyretic, analgesic and anti-inflammatory properties offered by Naproxen, while undesired adverse effects such as gastrointestinal upset and renal toxicities are linked to the COX-1 enzyme.

Preformulation Study

Preparation of naproxen standard solutions: An amount of 1.15 mg of naproxen was accurately weighed and placed in a 10 mL brown-colored volumetric flask. Methanol was added to volume to make the concentration of the stock solution exactly 500 μ M. Samples of 100, 200, 500, 1000 and 2000 μ L of the stock solution were respectively transferred to 10 mL brown-colored volumetric flasks. To each flask, 500 μ L of indomethacin in methanol of 25 μ M concentration was added as the internal standard and diluted with methanol to volume. The concentrations of the five standard solutions were 5.0, 10, 25, 50 and 100 μ M, respectively. The samples were filtered by 0.45 μ m Millipore membranes, and the filtrates were then subjected to HPLC analysis (Re et al. 2009).^[31]

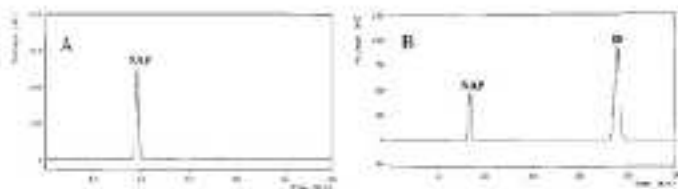


Figure 1.1: HPLC chromatograms of Naproxen (NAP) in methanol: (A) standard solution; (B) NAP with Indomethacin (IN) as the internal standard.

Evaluation Parameter

Bulk Density

Apparent bulk density (BD) was determined by placing presieved drug excipients blend into a graduated cylinder and measuring the initial volume (V_1) weight of powder (W). The bulk density was calculated using the formula

$$\text{Bulk Density (B.D)} = W / V_s$$

Tapped Density

The measuring cylinder containing known mass of blend was tapped for a fixed number of taps. The minimum volume (V_t) occupied in the cylinder and the weight of powder (W) was measured. The tapped density was calculated using the formula.

$$\text{Tapped Density (T.D)} = W / V_t$$

Angle of repose

Angle of repose (α) was determined by using funnel method. The blend was poured through a funnel that can be raised vertically until a maximum cone height (h) was obtained. The radius of the heap (r) was measured and angle of repose was calculated.

$$\alpha = \tan^{-1} (h/r)$$

Flowability	Angle of repose
Excellent	25-30
Good	31-35
Fair	36-45
Poor	45-55
Very poor	56-65
Very very poor	>66

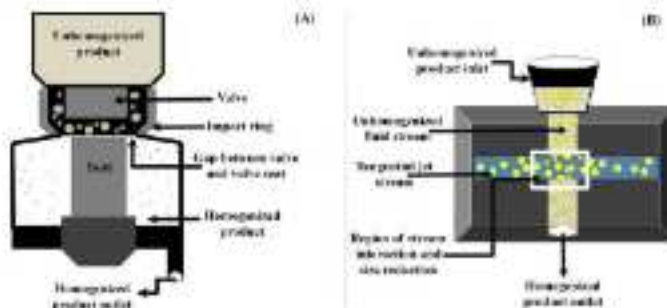
Methods of Preparation

- (1) High energy input methods.
- (2) Low energy input methods, and
- (3) Miscellaneous methods.

Hot HPH Technique: This is the most widely used method for industrial production of various lipid-based formulations such as microemulsions, liposomes, SLNs, and NLCs. In the case of nanoparticles production, the liquid lipid (used in the case of preparation of parenteral emulsion) is replaced by high speed stirring to form the preemulsion. The preemulsion thus formed is subjected to ultrasonication, followed by nano-sizing using a piston-gap homogenization principle or a jet-stream homogenization principle to form a hot colloidal emulsion, which is then cooled to room temperature, sub-zero temperatures or refrigerated to cause recrystallization of the lipid phase, thus forming the. The piston-gap homogenizers cause particle size reduction by forcing the macrosuspension/preemulsion through a small gap (of a few microns). The cavitation shear forces and impaction forces act on the particles to cause their size reduction. Whereas in the case of the jet-stream homogenizers, the size

reduction occurs due to impact forces generated by the collision of two high velocity streams. The formed nanoparticles exhibit an average particle size of 30–400 nm(Humberstone et al, 1997).^[34]

Cold HPH technique: This modified homogenization method is called "high pressure milling of liquid suspension". Mechanism of formation of nanoparticles through cold HPH technique: A lipid melt is obtained by heating solid lipids (in the case of SLNs) or a mixture of solid lipid and liquid lipid (in the case of NLCs) at 5°C above the melting point of the solid lipids. A drug lipid premix is obtained on dissolving dispersing the drug in the previously made lipid melt. This drug lipid premix is rapidly solidified using dry ice or liquid nitrogen to favor drug.



Schematic diagram of (A) piston-gap homogenization principle and (B) a jet-stream

Homogenization principle

Entrapment and stabilization in the lipid matrix: The solidified lipid melt is then subjected to milling/grinding to form microparticles. The obtained microparticles are then allowed to disperse in cold aqueous surfactant solution using high speed stirrer. The dispersion thus obtained is passed through the HPH to reduce the size of microparticles to nanorange for the formation of nanoparticles. The cold HPH method requires harsher homogenization conditions compared to the hot homogenization method as heating is not involved. The hot HPH technique has shown better results, compared to the cold HPH, as far as the monodispersity and particle size uniformity is concerned(Humberstone et al, 1997).^[34]

High shear homogenization technique

This method is similar in principle to that described by Speiser (1986) for the preparation of lipid nanoparticles for oral administration. This method involves the formation of emulsions by high shear mixing of hot lipid phase and hot aqueous surfactant phase at about 5000/25,000 rpm, at a temperature above the melting point of lipids. The high shear forces generated between rotor and the stator causes breakdown of the emulsion globules (Hamberhouse et al., 1997).²⁴

Electro-spray technique

This is a comparatively newer method for producing nanoparticles. A solution of the lipid drug mixture is prepared by dissolving them in aliphatic alcohol. This lipid mixture solution is sprayed through a metallic syringe with a cone-jet nozzle attached to a high voltage power supply. High interfacial tension and electrical forces results in generation of small homogeneous droplets. The droplets loose the solvent while passing through the electrical field due to evaporation, thus forming powder of nanoparticles. These highly charged powdered nanoparticles are collected by a metal foil that acts as a counter electrode. The technique requires optimization of liquid flow rate and the applied voltage according to the properties of the liquid in order to generate the nanoparticles of desired particle size and charge (Bennet et al., 2011).²⁵

Development of tablets

Naproxen solid lipid nanoparticle (NAP-SLN) tablets were prepared by the wet granulation method. All the excipients, with the exception of magnesium stearate and talc were thoroughly mixed in a tumbling mixer for 3 min and wetted in a granulating fluid PVP isopropyl alcohol. Accurate quantity of drug and polymers were weighed according to formula shown in Table 4.3.

The wet mass obtained was passed through sieve #16 and granules were dried at 60°C for 2 hours. The dried granules were passed through sieve #22 and these granules were lubricated with a mixture of magnesium stearate and talc (2:1) and the biopolymer chitosan was added in the mixture. The tablets were prepared using an electrically operated punches machine. Compression was performed after granulonaprocess with a single punch press applying a compression force of a 9 KN (preliminary work) or 12 KN (experimental design), equipped with a 3 mm concave punch. For the preliminary work, batches of 10 tablets were prepared. Each batch of experimental design consisted of 10 tablets (drug content in the tablet was 15

mg). Six batches were prepared for each formulation and the compositions of different batches of Naproxen tablets are given in Table below. The compressed tablets were evaluated for average weight & weight variation, thickness, diameter and content uniformity, hardness, friability (Xu et al. 2011)¹⁴².

Composition of tablets

Ingredients	Formulation code (Quantity in mg)								
	F-1	F-2	F-3	F-4	F-5	F-6	F-7	F-8	F-9
NAP-SLN	100	100	100	100	100	100	100	100	100
Chitosan	180	150	150	140	120	120	130	140	140
Pvp	56	56	56	56	60	60	56	56	60
Sodium Bicarbonate	80	80	80	75	72	72	80	90	10
Magnesium Stearate	8	12	8	10	12	12	8	10	12
Talc	6	6	46	6	4	6	6	6	6
St S Powder	4	6	3	7	6	6	7	6	7

Evaluation of tablets

Hardness

The hardness of a tablet is indication of its strength. It is tested by measuring the force required to break the tablet across the diameter. The force is measured in kg and the hardness of about 4 kg is considered to be satisfactory for uncoated tablets. Monsanto hardness tester is used for this purpose. The hardness of 6 tablets was measured and the average hardness was calculated (Mehmert et al. 2007)¹⁴³.

4.1.1. Friability test

Friability is the loss of weight of tablets in the container due to removal of fine particles from their surfaces. Friability test is carried out to assess the ability of the tablet to withstand abrasion in packing, handling and transport. Electrolab friability tester was used for finding out the friability of the tablet. A number of tablets (6) were weighed accurately and placed in the chamber of the apparatus. After 100 rotations, the tablets were taken out from the apparatus, re-dusted and weighed. The loss in weight indicates the friability of the tablets. A maximum friability of 1% is acceptable for tablets as per Indian Pharmacopoeia (IP). Percentage friability was determined by using the formula given below.

$$\% \text{ friability} = (W_1 - W_2 / W_1) \times 100$$

Where,

W₁ = weight of tablets before test

W₁ = weight of tablets after test

Dissolution Testing

The prepared tablets were evaluated for in-vitro drug release studies using with Auto sampler. The dissolution of core tablets is carried out under following conditions. The results obtained are tabulated and used for selection of best formulation. The results were given in Table below for Nitroglycerine (Lachman et al. 1989).⁴²⁾

RESULT AND DISCUSSION

5.1. Drug Identification Test

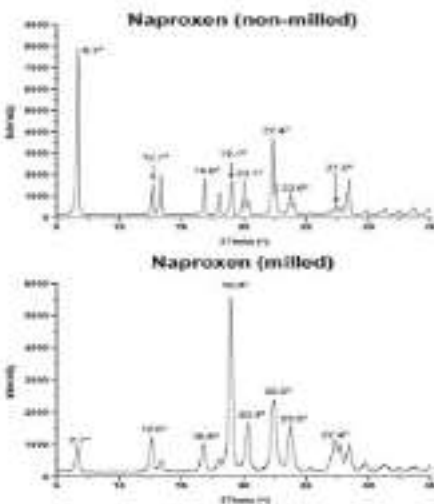
5.1.1. Solid State Characterization

In addition to the co-milled binary mixture of naproxen and cimetidine, the two single components were milled separately for comparison. The X-ray diffractogram of cimetidine (Form A) shows sharp after milling, suggesting the formation of amorphous cimetidine. This finding is supported by DSC, revealing a glass transition phase at 36.1±2.0 °C (Fig. 1) and Table 1) Although not directly comparable a previous study investigated the effects of milling metastable cimetidine (Form B) for 10 h using a mortar mill. In that study, milling induced a solid-state transition into the stable Form A with a concomitant formation of amorphous material. It is, however, not known whether the amorphization in that study proceeded through the stable (Form A) or metastable (Form B) polymorph. Naproxen presents a different case, as an amorphous phase is not easily formed upon milling. From (Fig. 5.1) it can be seen that naproxen is retained in a crystalline state even after milling for 60 min at 4 °C, and the unaltered position of diffractions in the X-ray diffractograms suggest that the same crystal form of naproxen is present in the non-milled and milled material. The discrepancy between diffraction intensities of non-milled and milled material is attributed to preferred orientation effects, while the minor peak shift and peak broadening could be due to a slight disordering of the crystals upon milling. The inability to form an amorphous form of naproxen by cold milling was not unexpected (Zecchi et al. 1984).⁴³⁾ Gupta et al. found that milling naproxen for 48 h at 25 °C did not induce any change in the crystal lattice. In contrast, amorphous naproxen prepared by quench cooling showed a glass transition at 6.2±0.6 °C (Table 3). Hence, after 60 min of milling, the powder temperature of naproxen (25 °C) was above the T_g, which led to no amorphization. This is in contrast to cimetidine where the powder temperature (25 °C) was below the T_g (36.1±2.0 °C), thus allowing amorphous formation. (Fig. 5.1) shows the XRPD data for co-milled mixtures of naproxen and cimetidine

at 1:2, 1:1, and 2:1 molar ratios. The lack of crystalline peaks and the detection of a single Tg for each sample (Figs. 12 and 11, respectively), confirm the formation of amorphous material at all three ratios. The Tgs for the three mixtures vary from 31.5 °C to 40.2 °C i.e. they are close to the Tg of amorphous cimetidine and, surprisingly, much higher than the Tg of quench-cooled naproxen (Table 5.1). Furthermore, the mixture with an excess of cimetidine (the 1:2 ratio) has the highest Tg (40.2 °C), while the 2:1 mixture, having naproxen as the excess component, has the lowest Tg (31.1 °C) (Table 5). A similar pattern was also observed in the binary mixtures of indomethacin and amitriptyline-HCl prepared by co-milling at various ratios. It was found that the newly observed Tg, relative to other binary mixtures, tends to be closer to the Tg of the component presence in excess within the mix. The Tgs also showed good correlation between the experimental and calculated (using Gordon-Taylor equation) values (Hsu et al., 2006).^[31]

Table: 5.1 Glass transition temperatures of mixtures and single components determined by DSC and calculated values using the Gordon-Taylor equation.

Sample	Tg (°C) - Experimental	Tg (°C) - Calculated
Naproxen (NAP)	6.2±0.6	N.A.
Cimetidine (CIM) (milled)	36.1±2.0	N.A.
(1:2) NAP-CIM	40.2±1.1	14.0
(1:1) NAP-CIM	34.5±0.3	10.7
(2:1) NAP-CIM	31.5±0.7	8.6



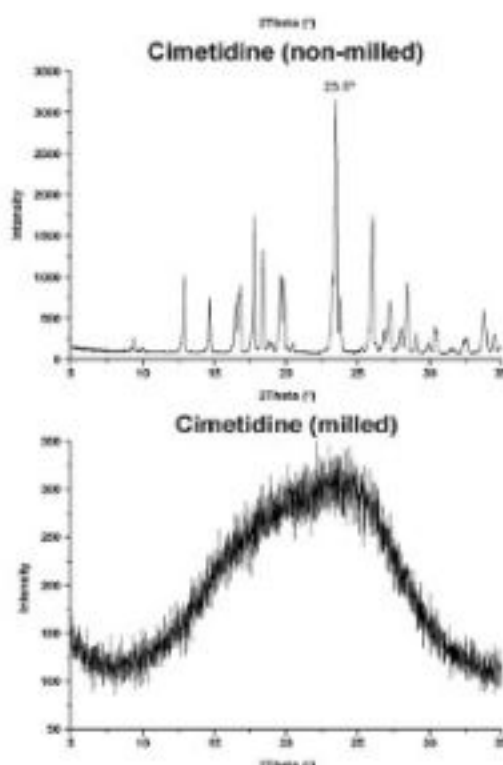
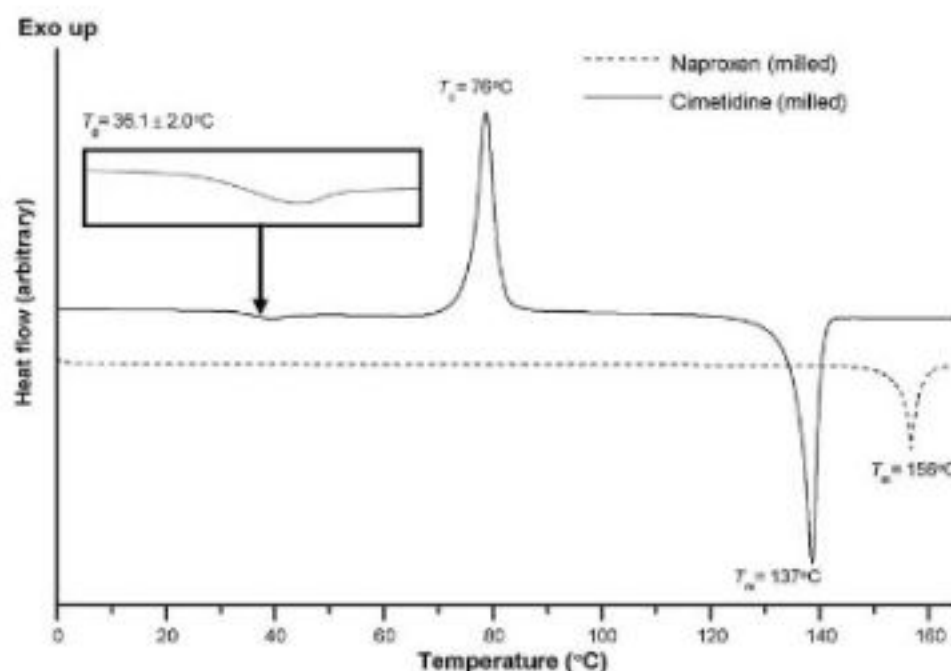


Fig.5.1: X-ray powder diffractograms of naproxen before and after milling for 60 min at 4 °C.



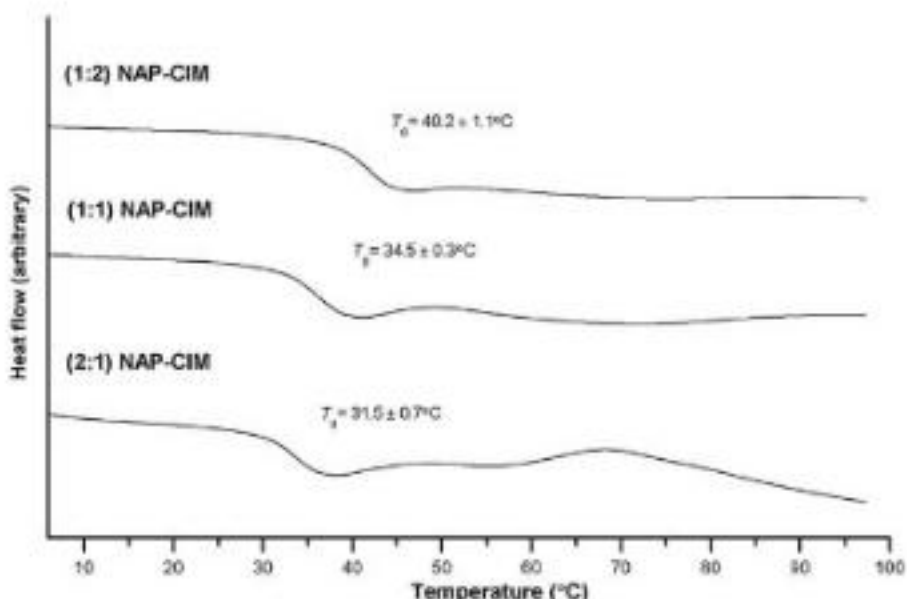
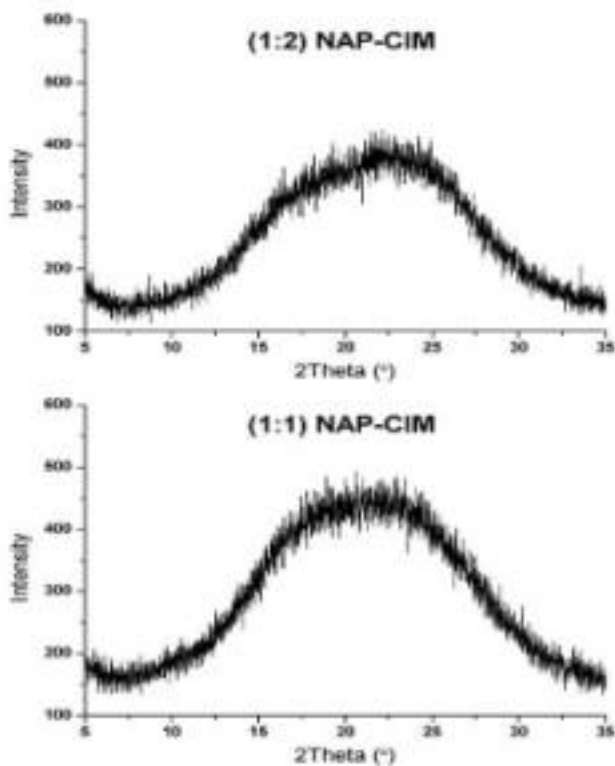


Fig. 5.2: DSC thermograms of milled naproxen and cimetidine and co-milled binary mixtures. The T_g of amorphous cimetidine has been enlarged to improve clarity.



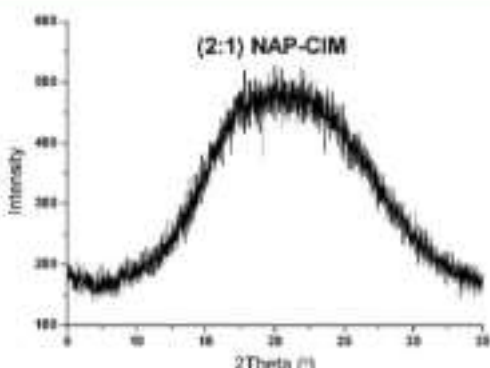


Fig. 5.3: X-ray powder diffractograms of co-milled naproxen-cimetidine (NAP-CIM) binary mixtures at three different ratios.

5.2. Physical stability testing

Results from the physical stability study are shown in (Fig. 5.4). It was found that the 1:1 amorphous mixture is the most physically stable sample after 33 days storage at all three temperatures, as a halo pattern could still be observed (Fig.5.4; 1:1 naproxen-cimetidine). The 2:1 sample, in contrast, is stable at 4 °C, while traces of crystalline naproxen, the excess component, are found at 25 °C. At 40 °C crystallization of naproxen is more pronounced. Surprisingly, although the 1:2 sample has the highest T_g (40.2 °C), traces of crystalline cimetidine are detected at all three temperatures (Helena Amaral et al, 2001).^[48] This kind of discrepancy between experimental T_{gs} of the amorphous mixtures and their physical stability has also been observed previously by our group in an indomethacin-ranitidine-HCl study. Here, in spite of not having the highest T_g, the 1:1 mixture of indomethacin and ranitidine-HCl was still found to be the most stable amorphous phase. Combined with the results from this study, these findings indicate that the stability of amorphous systems is governed not only by bulk-level phenomena but also by interactions at the molecular level. In addition, the 1:1 co-milled sample remained amorphous after 186 days of storage (approximately 6 months) at all three storage temperatures. X-ray diffractograms for this long-term stability study are provided in Supporting Information (Hsu et al, 2006).^[51]

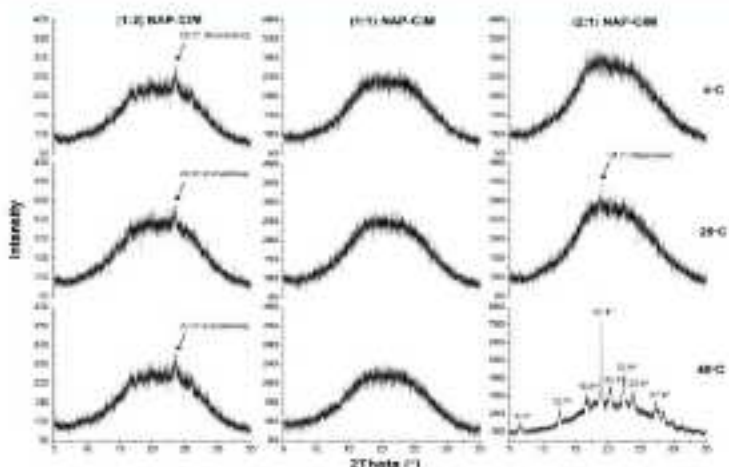


Fig. 5.4: X-ray powder diffractograms of co-milled naproxen-cimetidine (NAP-CD) samples stored for 33 days at 4 °C, 25 °C and 40 °C under dry conditions (silica gel). The observed peaks associated with the 2:1 sample at 40 °C are all related to the crystallization of naproxen (see Fig. 11).

5.3. Intrinsic dissolution testing

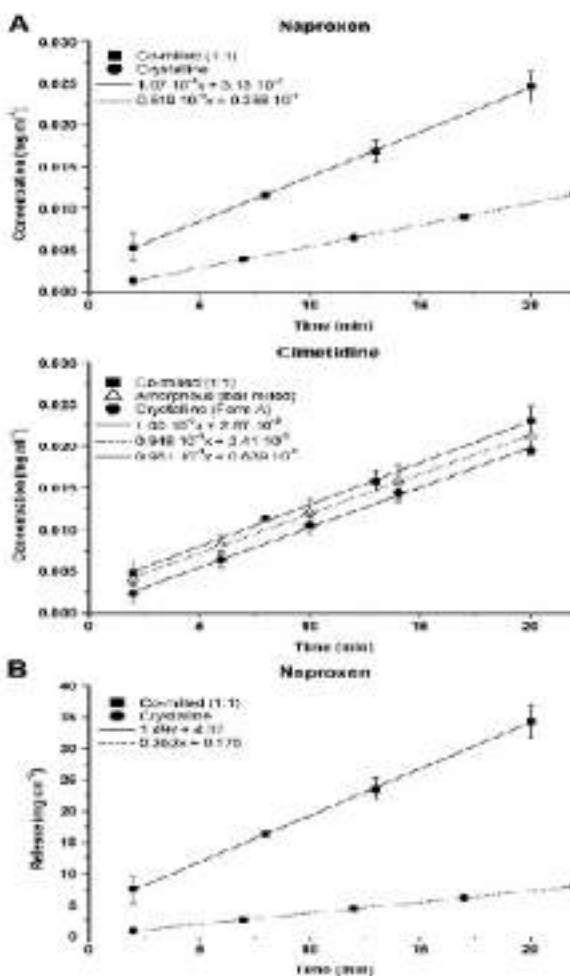
With reference to the stability study, it is obvious that the 1:1 co-milled sample carries the highest formulation potential of all the ratios investigated. This forms the rationale to further explore the amorphous 1:1 binary system by means of intrinsic dissolution testing. Shows the concentration-time profiles (mg ml^{-1}) for the two drugs in the co-milled sample as well as for the pure drugs. It was not possible to obtain meaningful dissolution profiles of a 1:1 physical mixture of crystalline naproxen and crystalline cimetidine, as the compact disintegrated within less than 5 min into the dissolution setting. This was not the case for the co-milled sample, which remained intact throughout the entire dissolution experiment. Most notable in fig. is the good linear fit for all five profiles, suggesting that the surface area does not change drastically over the course of the dissolution study. The saturation solubilities for naproxen and cimetidine in phosphate buffer are reported to be approximately 6 mg ml⁻¹ (37 °C, pH 7.0) and 19 mg ml⁻¹ (37 °C, pH 7.2), respectively. The dissolution system is thus undersaturated with respect to both components, and no precipitation from solution would be expected. To calculate release-time profiles (mg cm^{-2}) for the co-milled samples, an estimate

on the accessible surface area for each drug in the binary compact is model. The co-compact contains 490 mg amorphous ibuprofen corresponding to approximately 191 mg aspirin and 209 mg acetaminophen (1:1 molar ratio). Using the theoretical powder densities of 1.260 and 1.398 g cm⁻³ for aspirin and acetaminophen, respectively, the theoretical volume of each weighed amount amorphous ibuprofen is calculated as 0.151 mL for ibuprofen and 0.100 mL for acetaminophen. Hence, assuming a homogeneous mixture of the two drugs in the 1:1 co-compact sample, the total surface area of 1.33 m² for the binary system is (initially) comprised of 49% ibuprofen and 51% acetaminophen, i.e., 0.644 m² and 0.685 m², respectively. In contrast, the surface area of the pure sample compact is 1.33 m². Assuming that the surface area remains constant throughout the dissolution study the relative dissolution rate (Eqn no. 7) may now be calculated as depicted in Fig. 2B. Crystalline acetaminophen and ibuprofen have intrinsic dissolution rates (IDRs) of 0.162 and 0.664 mg cm⁻³ m⁻¹ s⁻¹, respectively (Fig. 1B and Table 4); their sum is roughly in line with results obtained by Yu et al. For co-compact ibuprofen there is a significant, approximately four-fold gain in IDR compared to its pure crystalline counterpart. The estimated and constant dissolution rate profiles for ibuprofen in the co-compact sample does not crystallize during dissolution. In the case of acetaminophen it was possible to prepare compacts above crystalline form (Figs A) as well as pure acetaminophen (assuming this to expand the compact). Surprisingly, there is no significant difference in the IDRs of pure amorphous and crystalline acetaminophen (95% confidence level; Table 5.2). XRPD confirmed that the compact of amorphous acetaminophen had not crystallized as a result of recrystallization (results not shown). Rather, the acetaminophen can sublime in the absence of the ibuprofen for amorphous acetaminophen (0.63 mg cm⁻²) and in crystalline material (0.072 mg cm⁻²). This higher order for amorphous acetaminophen may indicate an initially higher dissolution rate (below 1 min), reflecting the high solubility of the amorphous material, followed by recrystallization into a less soluble polymorph. Thus, the two profiles would eventually be parallel to each other. A similar phenomenon has been observed for amorphous ibuprofen and acetaminophen, where the initial dissolution advantage was not due to a greater increase in the degree of crystallization during dissolution. Hence, this suggests that pure amorphous acetaminophen may not sublime during dissolution in phosphate buffer. Co-compact acetaminophen, on the other hand, shows very promising dissolution characteristics. The IDR is improved two-fold over the crystalline material (significant at the 95% confidence level; Table 5.2). This gives further evidence that the solid-state interaction between the two drugs in the amorphous binary system is strong enough to prevent structure rearrangement of ibuprofen and acetaminophen molecules during dissolution. Consequently, enhanced dissolution rates are

observed for both drugs. As for pure amorphous cimetidine, there is a positive shift in offset (i.e., at 0 min) for both analytes in the co-milled sample (Manivannan et al., 2010).⁵² The observed increase in dissolution rate confirms that these-milled-sample remained amorphous throughout dissolution testing, and recrystallization is therefore not the reason for the higher offset in the dissolution tests. We speculate that it might be due to the higher hygroscopicity of the amorphous material (confirmed physically by the stickiness of the amorphous material during preparation). This may potentially lead to a rapid adsorption of water during the first few minutes of the dissolution experiment thereby yielding an initially faster dissolution rate. Extended-dissolution testing (120 min) as well as physical inspection of the compact after dissolution testing corroborated that the 1:1 co-milled sample remained amorphous during testing. The IDRs of naproxen and cimetidine in the co-milled sample (1.49 and 1.51 mg cm⁻², respectively) are not significantly different (95% confidence level; Table 5.2). But differently their release is synchronized, suggesting an inter-dependent controlled release of the two drugs from the compact. Taking into account the 1:1 solid-state interaction between the imidazole ring of cimetidine and the carboxylic acid of naproxen as well as the stability of the co-milled-amorphous system upon dissolution, this inter-dependency is not completely unexpected; however, remains an interesting finding. A pass-wax solvation process is believed to be the reason for the non-synchronous release; i.e., solvation of one cimetidine molecule leads to one non-bound naproxen molecule now having an exposed hydrophilic moiety (the carboxylic acid) accessible to solvation, and vice versa. The use of amorphous binary systems prepared by mechanical activation may present an alternative approach to synchronized release of drug-drug formulations, without relying on the introduction of a third component, for example a polymer. Taking into account that both drugs are intended for immediate-release, and that no signs of recrystallization were noticed during extended intrinsic dissolution study (see Supporting Information), it is reasonable to assume that bioavailability would not be decreased due to recrystallization in *in vivo* conditions either. Further studies on the naproxen-cimetidine binary system as well as other amorphous model systems are needed to explore the full potential of this formulation strategy. Such an investigation could include *in-situ* solid-state monitoring of the compact during dissolution, e.g., by Raman spectrometry, in order to elucidate the connection between solid- and solution-state phenomena. This would also serve as the basis for addressing the behavior of such coamorphophases in more complex formulations that include other excipients (Manivannan et al., 2010).⁵²

Table 5.2: Intrinsic dissolution rates (IDRs) of naproxen and cimetidine along with results from the t-test performed at the 95% confidence level.

API	Description	Intrinsic dissolution rate (mg cm ⁻² min ⁻¹)	t-test				
			X	X			
Naproxen	Co-milled	1.49±0.108	X	X			
	Crystalline	0.352±0.016			X		
Cimetidine	Co-milled	1.32±0.104	X		X	X	
	Amorphous (milled)	0.643±0.068			X		X
	Crystalline (Form A)	0.669±0.038				X	X
Significantly different (95% confidence level)			Yes	Yes	Yes	Yes	No



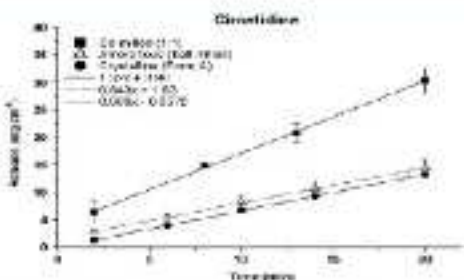


Fig. 5.5: Intrinsic dissolution profiles for naproxen and cimetidine from the co-milled (1:1) sample and for single components at pH 7.2, 37 °C and 50 rpm rotation speed. Conversion of (A) concentration-time profiles to (B) release-time profiles has been performed under the assumption that the co-milled sample is homogeneous and that the surface area of naproxen and cimetidine stays constant throughout the dissolution study.

REFERENCES

1. N. Poonia, R. Khatri, V. Lather, D. Pandita, Nanostructured lipid carriers: versatile oral delivery vehicle, *Future Science OA*, 2016; 2: FSO135.
2. Stegeman, F. Leveiller, D. Franchi, H. de Jong, H. Lindemans, When poor solubility becomes an issue: from early stage to proof of concept, *Eur. J. Pharmaceut. Sci.*, 2007; 31: 249e261.
3. C.A. Lipinski, F. Lombardo, B.W. Dominy, P.J. Feeney, Experimental and computational approaches to estimate solubility and permeability in drugdiscovery and development settings, *Adv. Drug Deliv. Rev.*, 2001; 46: 3e25.
4. C.A. Lipinski, Drug-like properties and the causes of poor solubility and poorpermeability, *J. Pharmacol. Toxicol. Meth.*, 2000; 44: 235e249.
5. S. Yeramun, S. Patel, P. Sharma, A. Bhargava, Design & development of solidself micro-emulsifying osmotic drug delivery system for irradipine, *J. Drug Deliv. Therapeut.*, 2014; 26:e11.
6. H.D. Williams, N.L. Trevaskiss, S.A. Chapman, R.M. Shanks, W.N. Chapman, C.W. Pouton, C.J. Porter, Strategies to address low drug solubility in discovery and development, *Pharmacol. Rev.*, 2013; 65: 315e499.
7. L. Di, E.H. Kems, G.T. Carter, Drug-like property concepts in pharmaceutical design, *Curr. Pharmaceut. Des.*, 2009; 15: 2184e2194.

8. J. Hunt, M. Kneer, A relation between the chain length of fatty acids and speeding up of gastric emptying. *J Physiol*, 1968; 194: 327e336.
9. N. Tajeswari, N. Hushavi, T. Tyutina, V. Gowri, V.P. Raju, Lipid based drug delivery system for enhancing oral bioavailability: contemporary review. *J. Global Trends Pharmaceut. Sci*, 2014; 5: 2074e2082.
10. P. Gerzhovcovich, A. Hoffman, Effect of a high-fat meal on absorption and disposition of lipophilic compounds: the importance of degree of association with triglyceride-rich lipoproteins. *Eur J Pharmaceut. Sci*, 2007; 32: 24e32.
11. E. Balkir, N. Aslano, A.V. Khan, Food-drug interaction. *Oman Med. J*, 2011; 26: 71e83.
12. R. Ghadi, N. Daud, DCS class IV drugs: highly toxicous candidates for formulation development. *J. Contr. Release*, 2017; 248: 71e95.
13. K. Cerpniak, A. Znalez, M. Ga spitz, F. Vre cer, Lipid-based systems as promising approach for enhancing the bioavailability of poorly water-soluble drugs. *Acta Pharm*, 2012; 62: 427e443.
14. D.G. Terroux, D.M. Kept, F.S. Nielsen, A. Mullertz, Clinical studies with oral lipid-based formulations of poorly soluble compounds. *Therapeut. Clin. RiskManag*, 2007; 3: 591.
15. K. Ibranin, R.P. Gengwani, A.T. Sazgarnavie, S. Jam, Oral delivery of anticoagulants: challenges and opportunities. *J. Contr. Release*, 2013; 170: 15e40.
16. H. Narvestad, R. Bela, S. Arora, Lipid-based drug delivery systems. *J. Pharmaceut*, 2014.
17. R.H. Miller, M. Radke, S.A. Waring, Solid lipid nanoparticles (SLN) and nanosstructured lipid carriers (NLC) in cosmetic and dermatological preparations. *Adv. Drug Deliv. Rev.*, 2002; 34: S121eS137.
18. M.C. Carey, D.M. Small, C.M. Shiu, Lipid digestion and absorption. *Annu. Rev. Physiol*, 1993; 45: 651e677.
19. S. Chakrabarty, D. Shukla, B. Mohra, S. Singh, Liposomes: emerging platform for oral delivery of drugs with poor bioavailability. *Eur. J. Pharm. Biopharm*, 2009; 73: 1e15.
20. C.J. Poste, N.L. Tsovalkaia, W.N. Clamanas, Lipids and lipid-based formulations: optimizing the oral delivery of lipophilic drugs. *Nat. Rev. Drug Discov*, 2007; 6: 231e248.
21. J.E. Stoggers, U. Hornell, P.J. Stafford, M.C. Carey, Physical-chemical behavior of dietary and biliary lipids during intestinal digestion and absorption. I. Phase behavior and aggregation state of model lipid systems prepared aftergastric duodenal contents of healthy adult human beings. *Biochemistry*, 1990; 19: 2018e2040.

22. O. Hennell, J.E. Stoggs, M.C. Coey, Physical-chemical behavior of dietary and biliary lipids during intestinal digestion and absorption. I. Phase analysis and aggregation states of luminal lipids during duodenal fat digestion in healthy adult human beings, *Biochemistry*, 1990; 29: 2041e2056.
23. Z. Zhang, F. Guo, S. Jiang, L. Chen, Z. Lin, H. Yu, Y. Li, Bile salts enhance transmucosal absorption of lipophilic drug loaded lipid nanoparticles: mechanistic and effect in rats, *Int. J. Pharm.* 2013; 452: 174e181.
24. B. Sanjala, F.M. Shah, A. Javed, A. Alta, Effect of galactosamer 138 on lymphatic uptake of carboxylic acid-modified lipid nanoparticles for bioavailability enhancement, *J. Drug Target*, 2009; 17: 239e256.
25. E. Rogez, F. Lagorce, E. Gariel, J-P. Bourrat, Lipid nanoparticles improve paclitaxel transport throughout human intestinal epithelial cells by using vesicle-mediated transcytosis, *J. Control Release*, 2009; 140: 174e181.
26. B. Grutza, C. O'Donnell, Opportunities and challenges for oral delivery of hydrophobic versus hydrophilic peptide and protein-like drugs using lipid-based technologies, *Ther. Deliv.* 2011; 2: 1653e1659.
27. L. Kagan, A. Hoffman, Selection of drug candidates for gastrointestinal drug-formulation kinetics following continuous intraduodenal route of administration: a rat model, *Eur. J. Pharm. Biopharm.* 2003; 60: 238e246.
28. A. Elgari, I. Chernukov, Y. Aldeeb, A.J. Davis, A. Hoffman, Liposomes and nano-liposomes for delivery of poorly water soluble compounds, *Chem Phys. Lipids*, 2012; 165: 435e453.
29. O. Dangra, J.S. Bernstein, Emulsion formulations, in, Google Patents, 2013.
30. R. Martiz-Venegas, M.L. Rodriguez-Lagunes, P.A. Gerest, R. Ferrer, Monocarboxylate transporter 1 mediates 1,3-Hydroxy-(4-methylbutyric) branched-acid transport across the apical membrane of Caco-2 cell monolayers, *J. Nutr.* 2007; 137: 149e154.
31. D. Damjanovic, A.J. Shaw, A.T. Florence, Effects of some non-toxic surfactants on paracellular permeability in Caco-2 cells, *J. Pharm. Pharmacol.* 2000; 52: 157e162.
32. I.Z. Bent, Predicting drug disposition via application of a biopharmaceuticsdrug disposition classification system, *Basic Clin. Pharmacol. Toxicol.* 2010; 106: 162e167.
33. I. Midgley, K. Fitzpatrick, L.M. Taylor, T.L. Hooton, S.J. Henderson, S.J. Wright, Z.P. Cywinski, B.A. John, A. McSweeney, D.W. Boykin, Pharmacokinetics and metabolism of the prodrug DB289 (2, 3-bis [4-(N-methoxyamino)phenyl] fumarimide) in rat

- and monkey and its conversion to the antiprotozoal antifungal drug BB75 (2, 3-bis(4-guanylphenyl)triazen dihydromelamine). *Drug Metab Dispos*. 2007; 35: 951-967.
34. X. Rao, X. Ma, L. Si, L. Cao, H. Xiang, J. Qiu, A.D. Schimenti, G. Li. Pharmaceutical compounds inhibit cytochrome P450 activity in cell free systems and after systemic administration. *Eur J Pharm Biopharm*. 2008; 70: 279-288.
 35. R.J. Mountfield, S. Seneca, M. Schleifer, I. Walter, B. Bitter, Potenzial P. 14Ganoderen, D. Newpanzeri. *Futura Journal of Pharmaceutical Sciences*. 2016; xxv: 1-15.
 36. A.J. Hunterston, W.N. Chennar, Lipid-based vehicles for the oral delivery of poorly water soluble drugs. *Adv Drug Deliv Rev*. 1997; 25: 103-128.
 37. L.Z. Benet, F. Broccarelli, T.L. Oyrea, BDDCS applied to over 900 drugs. *AAPS J*. 2011; 13: 519-547.
 38. E.N. Gursoy, S. Bensz, Self-emulsifying drug delivery systems (SEDDS): improved oral delivery of lipophilic drugs. *Biomed Pharmacother*. 2004; 58: 171-182.
 39. T. Agarwal, K.C. Patkar, K.K. Savant, Development, evaluation and clinical studies of Acitretin loaded nanstructured lipid carriers for topical treatment of psoriasis. *Int J Pharm*. 2010; 401: 95-102.
 40. J. Vashishta, M. Tahirkhanvi, M.Y. Mohammad, Formulation and optimization of solid lipid nanoparticles of buspirone HCl for enhancement of its bioavailability. *J Liposome Res*. 2010; 20: 286-296.
 41. Y.-L. Lin, Z.-R. Huang, R.-Z. Zhao, J.-Y. Fang, Combination of calcipotriol and methotrexate in nanstructured lipid carriers for topical delivery. *Int J Nanomed*. 2010; 5: 117-126.
 42. K. Marimuthu, J.S. Reddy, V. Venkateswarlu, Solid lipid nanoparticles as drug delivery systems. *Methods Mol Exp Clin Pharmacol*. 2003; 27: 127-144.
 43. K. Marimuthu, V. Venkateswarlu, Pharmacokinetic tissue distribution and bioavailability of doxorubicin solid lipid nanoparticles after intravenous and intracardiac administration. *J Controlled Rel*. 2005; 107: 215-225.
 44. X.-m. Xu, Y.-s. Wang, R.-j. Chen, C.-l. Feng, F. Yao, S.-s. Tong, L. Wang, F. Yamashita, J.-n. Yu, Formulation and pharmacokinetic evaluation of temozolamide-loaded solid lipid nanoparticles for subcutaneous injection routes. *Chem Pharmaceut Bull*. 2011; 59: 260-266.
 45. I. Stecova, W. Menzert, T. Blaschke, B. Kleiser, B. Sovranekova, C.C. Zschiedrich, H. Seifert, H.G. Korting, K.D. Kramer, M. Schäfer-Korting, Cyproterone

- acetate loading to lipid nanoparticles for topical acne treatment: particle characterisation and skin uptake. *Pharmaceut. Res.* 2007; 24: 991e1000.
46. Lachman L, Lieberman HA, Kanig JL. *Pharmaceutical Dosage Forms-Tablets*. 2nd ed. Vol 1. New York: Marcel Dekker Inc, 1989; 13.
 47. Zecchi V, Rodriguez L, Tartarini A, Chiarini A, Valenti P. *In vitro* absorption studies on naproxen and its sodium and piperazine salts. *Pharm Acta Helv*. 1984; 59: 91-94.
 48. M. Helena Amaral, J.M. Sousa Lobo and D.C. Ferreira, Effect of hydroxypropyl methyl cellulose and hydrogenated castor oil on naproxen release from sustained release tablets. *AAPS PharmSciTech*. 2001, 2(2); article 6, 1-8.
 49. Palazzini E, Galli G, Babbini M. Pharmacokinetic evaluation of conventional and controlled release product of Naproxen. Drug under experimental and clinical research. 1990; 16(5): 243-247.
 50. US pharmacopoeia XXIII, Rockville, MD: US Pharmacopoeia Convention, 1995; 1054
 51. Higuchi T. Mechanism of sustained-action medication. Theoretical analysis of rate of release of solid drugs dispersed in solid matrices. *J Pharm Sci*, 1963; 52: 1145-1149.
 52. European Pharmacopeia. 3rd ed. Council of Europe, Strasbourg, 1997; 133-135.